Density Functional Theory Study of CsC_n^- ($n = 1-10$) Clusters

J. Y. Qi, L. Dang,† M. D. Chen,* W. Wu, and Q. E. Zhang

State Key Laboratory of Physical Chemistry of Solid Surface, Department of Chemistry, Center for Theoretical Chemistry, College of Chemistry and Chemical Engineering, Xiamen University, Xiamen 361005, People's Republic of China

C. T. Au

Department of Chemistry, Hong Kong Baptist University, Kowloon Tong, Hong Kong, People's Republic of China

Received: May 19, 2008; Revised Manuscript Received: October 03, 2008

In this paper, we report the design of numerous models of CsC_n^- ($n = 1-10$). By means of B3LYP density functional method, we carried out geometry optimization and calculation on the vibrational frequency. We found that the CsC_n^- ($n = 4-10$) clusters with Cs lightly embraced by C_n are ground-state isomers. The structures are composed of C_n^{2-} and Cs^+ with the former being electronically stabilized by the latter. When n is even, the C_n ($n = 4-10$) chain is polyacetylene-like. The CsC_n^- ($n = 1-10$) with even n are found to be more stable than those with odd n, and the result is in accord with the relative intensities of CsC_n^- ($n = 1-10$) observed in mass spectrometric studies. In this paper, we provide explanations for such trend of even/odd alternation based on concepts of the highest vibrational frequency, incremental binding energy, electron affinity, and dissociation channels.

1. Introduction

In the past decades, carbon clusters have been studied experimentally and theoretically; this is because detailed knowledge about the physical and chemical properties of these clusters is essential for understanding a large variety of chemical systems. Even before the development of fullerene chemistry, studies of small carbon clusters were of special interest due to their importance in combustion and pyrolysis, in formation and growth of fullerenes and nanotubes, and in astrophysical processes for the identification of species in interstellar and circumstellar media.[1,2] In outer space under quasi-collisionless conditions, carbon takes the highly stable, albeit highly reactive, form of linear chains in which the atomic orbitals are sp-hybridized; some of them may be terminated by hydrogen atoms or by heteroatom(s).[3] In recent years, the doping of carbon clusters with heteroatom(s) has received much attention because the addition of heteroatom(s) provides a means to stabilize the carbon chain. One might speculate the analogies and the interplay between the study of fullerenes and molecular systems that are detectable in outer space. The study of anionic clusters is of particular interest since photoelectron spectroscopy provides only indirect information on their structure;[4] also by means of secondary ionic emission or laser ionization, heteroatom−carbon C_nX^- clusters (X = an atom of main group, transition, or nonmetal element) can be fabricated.[5−9] One may obtain the earliest clues related to the geometrical structure of the species produced from the yield distribution of carbon clusters. For example, Gupta and Krishnamurthy produced CsC_n^- ($n = 1-10$) clusters in the sputter ion source by bombarding a graphite surface with 5 keV Cs^+ ions.[10] Indeed, the study of various types of atomic clusters has created tremendous interest among both experimentalists and theoreticians.

Due to interest of astrochemistry and the possibility of designing novel materials, heteroatom-doped anionic carbon clusters have been subject to extensive theoretical investigations. Numerous theoretical studies on similar systems have been conducted by a number of research groups using various levels of calculation. These investigations are summarized in Table 1.

In the generation of CsC_n^- ($n = 1-10$) clusters, Gupta and Krishnamurthy observed an odd/even pattern: the intensities of even-n species are distinctly larger than those of odd-n ones.[10] No account has been offered to explain this striking effect; up until now, only five CsC_7^- and nine CsC_9^- isomers have been studied (SCF, MP2, and CCSD level, by Dreuw and Cederbaum).[42] To explore the observation of Gupta and Krishnamurthy further, we designed a large number of structural models of CsC_n^- ($n = 1-10$) and performed geometry optimization and calculation on vibrational frequencies by means of the B3LYP density functional method. The geometrical structure and parameters, atomic charges, the highest vibrational frequency, incremental binding energy, electron affinity, and dissociation channels of the clusters were examined. On the basis of the results, we provide an explanation to why the even-n ground-state CsC_n^- ($n = 1-10$) isomers are more stable than the odd-n ones. The outcome can serve as a guideline for the synthesis of related materials as well as for future theoretical studies of carbon/cesium binary clusters.

2. Computational Method

During the investigation devices for molecular graphics, molecular mechanics, and quantum chemistry examination were used. First, a three-dimensional (3D) model of a cluster was designed using HyperChem for Windows on a PC computer;[43]

* To whom correspondence should be addressed. E-mail: mdchen@xmu.edu.cn.

† Present address: Department of Chemistry, Hong Kong University of Science and Technology, Clear Water Bay, Kowloon, Hong Kong, People's Republic of China.

10.1021/jp807039j CCC: $40.75
Published on Web 11/12/2008

TABLE 1: Theoretical Investigations on Heteroatom-Doped Carbon Anionic Clusters

cluster	level	authors
C_nN^- ($n = 1-13$)	HF	Wang et al. (ref 11)
C_nB^- ($n = 1 < 13$)	HF	Wang et al. (ref 12)
C_nP^- ($n = 1-13$)	HF	Liu et al. (ref 13)
AlC_n^- ($n = 1-11$)	HF	Liu et al. (ref 14)
C_nSe^- ($1 \le n \le 11$)	DFT/B3LYP	Wang et al. (ref 15)
C_nN^- ($n = 1-13$)	MP2, MP4	Zhan and Iwata (ref 16)
C_nB^- ($n = 1-7$)	MP2, MP4	Zhan and Iwata (ref 17)
C_nP^- ($n = 1-7$)	MP2, MP4	Zhan and Iwata (ref 18)
C_nN^- ($n = 1-7$)	DFT/B3LYP	Pascoli and Lavendy (ref 19)
C_nP^- ($n = 1-7$)	DFT/B3LYP	Pascoli and Lavendy (ref 20)
C_nP^- ($n = 3-9$)	DFT/BLYP	Fisher et al. (ref 21)
C_nX^- ($n = 1-10$, X = Na, Mg, Al, Si, P, S, or Cl)	DFT/B3LYP	Li and Tang (ref 22)
PbC_n^- ($n = 1-10$)	DFT/B3LYP	Li et al. (ref 23)
GeC_n^- ($n = 1-9$)	DFT/B3LYP	Cao et al. (ref 24)
RbC_n^- ($n = 1-10$)	MP2	Vandenbosch and Will (ref 25)
$Si_nC_m^-$ ($n + m \le 8$)	MD/DFT	Hunsicker and Jones (ref 26)
SiC_n^- ($n = 2-5$)	MP2, CCSD(T)	Gomei et al. (ref 27)
C_nH^- ($n \le 10$)	DFT/B3LYP	Pan et al. (ref 28)
AlC_n^- ($n = 1-7$)	DFT/B3LYP	Largo and co-workers (refs 29 and 30)
NaC_n^- ($n = 1-8$)	DFT/B3LYP	Redondo et al. (ref 31)
MgC_n^- ($n = 1-7$)	DFT/B3LYP	Redondo et al. (refs 32 and 33)
CaC_n^- ($n = 1-8$)	DFT/B3LYP	Redondo et al. (ref 34)
C_nCl^- ($n = 1-7$)	DFT/B3LYP	Largo et al. (ref 35)
TiC_n^- ($n = 1-8$)	DFT/B3LYP	Largo et al. (ref 36)
ScC_n^- ($n = 1-8$)	DFT/B3LYP	Redondo et al. (ref 37)
VC_n^- ($n = 1-8$)	DFT/B3LYP	Redondo et al. (ref 38)
CrC_n^- ($n = 2-8$)	DFT/B3LYP	Zhai et al. (ref 39)
C_nAs^- ($n = 1-11$)	DFT/B3LYP	Liu et al. (ref 40)
BeC_n^- ($n = 1-8$)	DFT/B3LYP	Chen et al. (ref 41)

the model was then optimized by MM+ molecular mechanics and extended Hückel semiempirical quantum chemistry. At the final stage, geometry optimization and calculation of vibrational frequencies were conducted using the B3LYP density functional method of Gaussian 03 package;[44] i.e., Becke's three-parameter nonlocal exchange functional with the correlation functional of Lee−Yang−Parr.[45,46] We employed a mixed basis set formed by the relativistic effective core potentials (RECPs) given by Hay/Wadt: the LanL2DZ basis sets[47−49] for cesium and the 6-311+G*//6-311G* basis sets for carbon atom(s). The geometry optimization and vibrational frequencies calculation were performed using the 6-311G* basis sets for carbon atoms and LanL2DZ basis set for cesium atom, whereas calculation of single-point energies was conducted using the larger 6-311+G* basis sets with diffuse functions for carbon atoms and LanL2DZ basis set for cesium atom. It has been pointed out that using geometries computed with more expensive basis sets does not necessarily lead to results of better accurracy.[50] All energies were calculated with zero-point energy (ZPE) correction; as the quality of employed method for calculation has very little effect on ZPE variation, all energies were calculated with ZPE correction at the B3LYP/6-311G* level. The optimized models were again displayed using HyperChem. The data of partial charges were analyzed with Gaussian natural bond orbital (NBO). All the calculations were carried out on SGI servers.

3. Results and Discussion

3.1. Geometrical Configuration. Because the possible structures of clusters are many, the identification of the ground-state ones is most important. The ground-state isomers of heteroatom(s)-doped carbon clusters may adopt different configurations. The linear configurations terminated by heteroatom(s) are rather common among stable isomers, e.g., C_nN^- ($n = 1-7$).[19] For C_nB ($n = 4-10$)[51] or C_nBe^{2-} ($n = 4-14$)[52] clusters, the linear configuration with a boron or beryllium atom located inside a carbon chain is the most stable. For C_nH^- ($n \le 10$) clusters, the configurations with a bent C_n chain terminated by a hydrogen atom are the most favorable.[28] In the cases of CsC_7^-, CsC_9^-, and $TiC_n^{\pm}$ ($n = 1-6$) clusters, isomers with a "lightly embracing" or "fan" structure have been suggested to be the most stable.[36,42]

At the beginning of the study, nothing was known other than the CsC_n^- formula. The assumption of a reasonable geometrical structure was the beginning of the optimization process. The adopted approach for the determination of geometries is based on comparing the total energy resulted from theoretical calculations. In order to reduce the chance of having the ground-state structures wrongly identified, we examined a huge number of models that are reasonable in chemical understandings. We studied models that are embraced, linear, cyclic, chainlike, branched, and propeller-like in structure. After geometry optimization, the total energies were compared for the determination of ground-state isomers; in this paper, those with imaginary frequency, high energy, and large spin contamination are excluded.

Displayed in Figure 1 are 12 major categories of CsC_n^- ($n = 1-10$). Belonging to category 1a are structures with the Cs atom lightly embraced by a C_n chain. Belonging to category 1b are structures also with the Cs atom lightly embraced but by a C_{x+y+1} subunit with an inside atom bonded to a $C_{n-x-y-1}$ branch. In category 1c are CsC_n ring structures. In category 1d are structures with the Cs atom placed next to a C_n ring. In category 1e are structures with the Cs atom placed next to a C_{n-x} ring bonded to a $-C_x$ chain. In category 1f are structures with the Cs atom placed next to a C_{n-x-y} ring with two of the ring atoms bonded to a C_x and a C_y chain individually. Belonging to category 1g are structures of linear C_n with a terminal Cs atom. Belonging to category 1h are structures of zigzag C_n chains with a terminal Cs atom. In category 1i are structures with the Cs atom placed between two branches of a "Y-shaped" C_n structure. The structures of category 1j are with the Cs atom connected to the terminal of a branch of a "Y-shaped" C_n. The isomers of category 1k are with the Cs atom placed between two branches of a carbon entity of propeller shape, whereas those of category 1l are with the Cs atom located next to a terminal atom of one of the carbon branches of propeller-like C_n. We found that the ground states of CsC_2^- and CsC_3^- are triangular and nearly triangular, respectively. For CsC_n^- ($n = 4-10$) clusters, the ground-state structures are those of category 1a.

The total energies, categories, relative energies of the most, second most, and third most stable isomers of CsC_n^- ($n = 4-10$) are shown in Table 2. Dreuw and Cederbaum examined the structure of five CsC_7^- and nine CsC_9^- isomers.[42] They also considered that the CsC_9^- of category 1a is the ground-state isomer (singlet, $^1A_1$ electronic state, C_{2v} symmetry). For CsC_7^-, the lightly embracing isomer ($^1A'$ electronic state) with C_s symmetry is considered by them to be the most stable. They pointed out that the triplet CsC_9^- ($^3A''$ electronic state) structure in the lightly embracing configuration is higher in energy, and the geometry optimization of it at the CCSD level led to

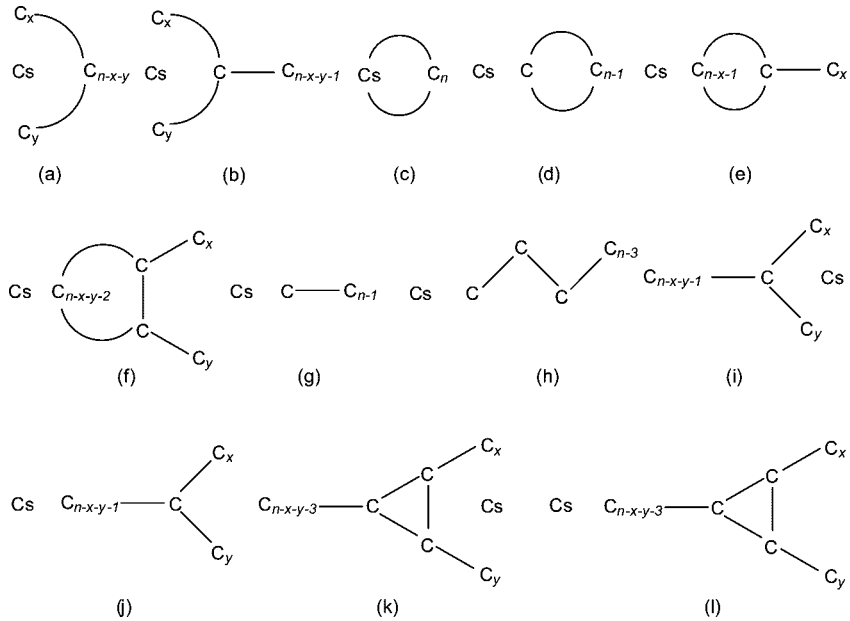

Figure 1. Twelve main categories of CsC_n^- ($n = 1-10$) structures (x, y denote numbers of carbon atom(s)).

TABLE 2: Total Energy (au), Category, and Relative Energy (kcal/mol) of the Most, Second Most, and Third Most Stable Isomers of CsC_n^- ($n = 4-10$)

cluster	category	total energy	relative energy
CsC_4^-	1a	−172.186036	0.00
CsC_4^-	1g	−172.158340	17.38
CsC_4^-	1d	−172.097508	55.55
CsC_5^-	1a	−210.250475	0.00
CsC_5^-	1k	−210.223249	17.08
CsC_5^-	1e	−210.157303	58.47
CsC_6^-	1a	−248.387090	0.00
CsC_6^-	1g	−248.338856	30.27
CsC_6^-	1k	−248.268537	74.39
CsC_7^-	1a	−286.447246	0.00
CsC_7^-	1i	−286.420773	16.61
CsC_7^-	1j	−286.415908	19.66
CsC_8^-	1a	−324.571375	0.00
CsC_8^-	1e	−324.428214	89.83
CsC_8^-	1d	−324.411542	100.30
CsC_9^-	1a	−362.633893	0.00
CsC_9^-	1k	−362.600417	21.01
CsC_9^-	1d	−362.526043	67.68
CsC_{10}^-	1a	−400.748515	0.00
CsC_{10}^-	1d	−400.609044	87.52
CsC_{10}^-	1d	−400.557281	120.00

fragmentation of C_9 into one C_5 and two C_2 units that are still bound to the Cs atom. The examination of possible triplet states of lightly embracing structures of the CsC_7^- isomer led to results analogous to those of CsC_9^- triplet states.[42] According to our calculation, the singlet CsC_9^- with $^1A_1$ electronic state (−362.628763 au) in the lightly embracing configuration (0.005130 au higher in total energy than triplet CsC_9^- (−362.633893 au)) is the second most stable. As for CsC_7^-, we obtained singlet ($^1A_1$ electronic state) and triplet ($^3B_1$ electronic state) isomers, both with lightly embracing configurations of C_{2v} symmetry. Being 0.007999 au higher in energy than the latter (−286.447246 au), the singlet isomer (−286.439247 au) is the second most stable. In other words, we obtained ground-state CsC_7^- and CsC_9^- isomers with geometry configuration similar to that of Dreuw and Cederbaum, but there was a discrepancy in the electronic state.

The singly occupied HOMO and HOMO−1 of CsC_7^- in the triplet ground state are displayed in Figure 2. One can see bonding character at the ends and antibonding character in the middle of the carbon chain. The association of Cs^+ with the conjugated backbone results in splitting of degenerate π orbitals.

We carried out QCISD calculation with the same basis set of B3LYP on ground-state CsC^- and CsC_2^- clusters. The QCISD energies for CsC^- and CsC_2^- are −57.448126 and −95.489194 au, respectively. The QCISD bond length for CsC^- is 3.218 Å, just a little bit shorter (0.012 Å) than that of B3LYP (3.230 Å). For CsC_2^-, QCISD bond lengths of Cs−C and C−C are 3.260 and 1.264 Å, respectively; compared to B3LYP bond lengths (3.095 and 1.270 Å); there is a difference of 0.195 Å for Cs−C but no discrepancy in C−C bond length. In the case of ground-state CsC_n^- ($n = 1, 3, 5, 7, 9$) isomers of triplet state, spin contamination $\langle S^2 \rangle$ values are 2.9154, 2.0169, 2.0485, 2.0911, and 2.1107, respectively, before annihilation of contaminants. They are 2.0065, 2.0001, 2.0013, 2.0050, and 2.0077, correspondingly, after annihilation. Such a small deviation should not have severe effects on our results in terms of an expected value of 2.0.

3.2. Geometrical Parameters and Atomic Charges. Depicted in Figure 3 are optimized geometrical configurations and NBO charges of ground-state CsC_n^- ($n = 1-10$). Together with the 2D graphic configurations (shown as real molecular models) are synchronized displays of 3D graphics, and according to 3D bond criterion, the solid lines denote the nature of chemical bonding. The geometrical details of ground-state CsC_n^- ($n = 1-10$) clusters are given in Table 3. According to the results, the Cs−C bond lengths exhibit essential characteristics of single or weak bonds. The Cs−C bonds represented by solid lines (in the 3.086−3.432 Å range) are single bonds, and those represented by dashed lines (in the 3.486−4.024 Å range) are weak bonds. According to Van Orden and Saykally, the bonding of small linear carbon chains could be either cumulene- or polyacetylene-like.[1] When n is even, we observed alternate short-and-long pattern of C−C length (short, 1.236−1.257 Å, and long, 1.338−1.348 Å) along the carbon chains of ground-state CsC_n^- ($n = 4-10$) isomers. When n is odd, such a display of short−long alternation tends to fade toward the center of the chain (short, 1.264−1.285 Å, and long, 1.307−1.338 Å). As

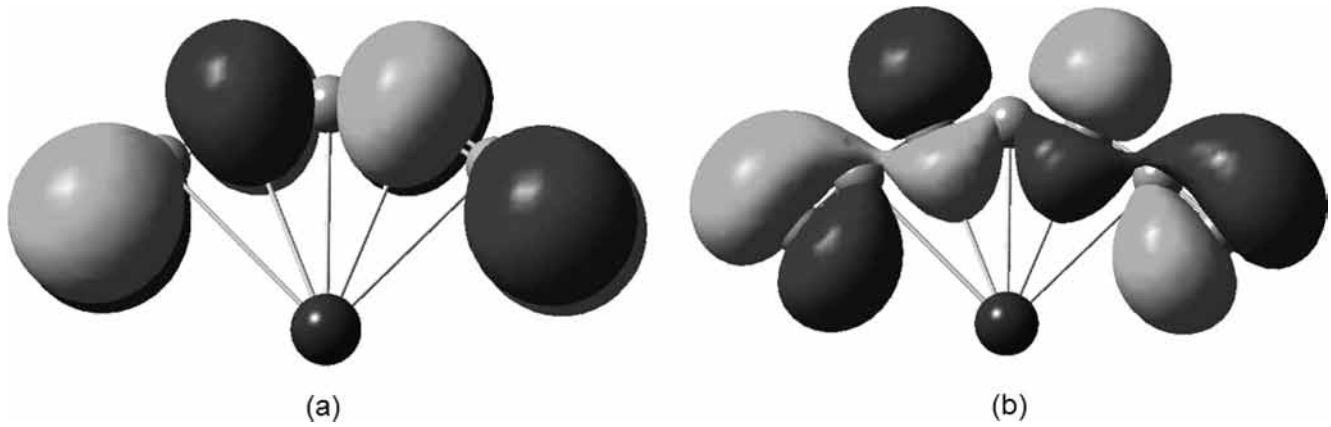

Figure 2. (a) HOMO and (b) HOMO−1 molecular orbitals for the ground-state CsC_7^- cluster.

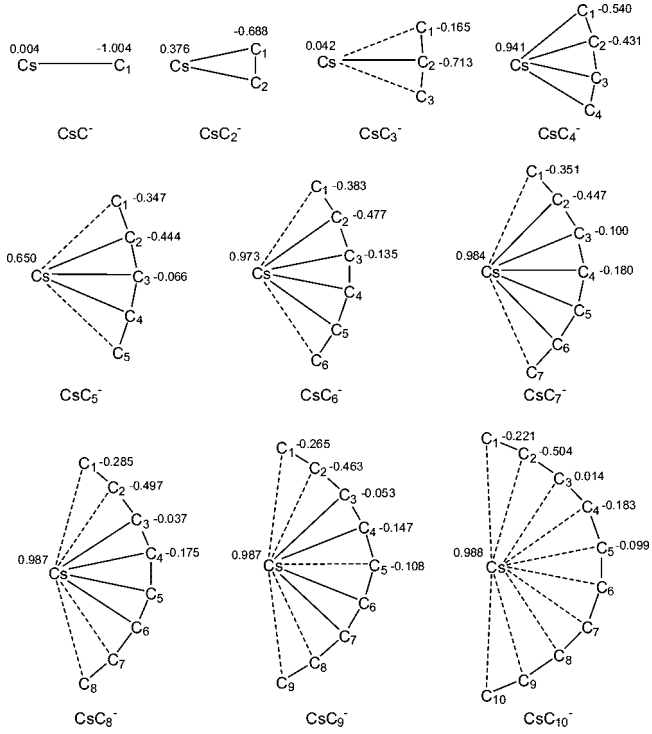

Figure 3. Optimized geometrical configurations and NBO charges of ground-state CsC_n^- (n = 1−10) clusters. (Solid lines are displayed according to 3D graphic bond criterion.)

an illustration, depicted in Figure 4 are the C−C bond lengths of ground-state CsC_9^- and CsC_{10}^- isomers versus the number of bonds (as counted from top to bottom in Figure 3, e.g., the C_1-C_2 bond length is plotted against "1" and so on). The carbon chain of CsC_{10}^- displays obvious short−long alternation and can be considered as polyacetylene-like. As for CsC_9^-, such short−long alternation is not apparent toward the center of the chain.

According to the NBO charges of CsC_n^- (n = 4−10) depicted in Figure 3, the positive charge is located at the cesium atom (in the range of 0.941−0.988). The majority of the negative charge is located at the ends of the carbon chain. It is interesting to note that the penultimate carbon atoms are more negative (−0.431 to −0.504) than those (−0.221 to −0.540) located at the ends. It can be considered that the CsC_n^- (n = 4−10) isomers are composed of a Cs^+ cation and a C_n^{2-} dianion. It is not surprising to find that the majority of negative charge is located at the terminal atoms of the carbon chain because such a distribution is most favorable in terms of minimization of Coulomb repulsion force. The strong force of Coulomb repulsion of a doubly charged anion would either enhance the emission of an electron or promote the decomposition of frame into two monoanionic fragments.[53] For C_nBe^{2-} (n = 4−14) clusters, the dianionic structures with the beryllium atom located inside the carbon chain are more stable than those with the beryllium atom located at one end of the chain. This is understandable as the interior beryllium atom plays a role of reducing Coulomb repulsion by separating the two negative charges.[52] The ground-state C_nS^{2-} (n = 6−18) are linear with the sulfur atom located at one end. The majority of negative charge is located at the sulfur atom as well as distributed on the two carbon atoms close to the other end. The structure of C_nS^{2-} (n = 6−18) is stabilized due to obvious reduction of the Coulomb repulsion force.[54] In ground-state CsC_n^- (n = 4−10), the large Cs^+ seems to be lightly embraced by C_n^{2-}, and the structure of the C_n frame reflects the geometry of the corresponding carbon dianion. The polarization pattern and the resulting geometries can be better understood in terms of electrostatic models. The Cs^+ cation prefers to interact with two or more negative centers rather than one. The ground-state geometries and the polarization pattern favor maximum yield of electrostatic energy and hence stabilization of negative charge.

The structures of aqua−cesium clusters $Cs^+(H_2O)_n$ (n = 1−8) are completely different from those of gas-state CsC_n^- (n = 4−10) clusters. In aqua−cesium clusters, water−water and cesium−water interactions influence the hydrogen-bonding structure of $Cs^+(H_2O)_n$ clusters.[55] In the case of cesium-doped carbon clusters CsC_n^- (n = 4−10), the Cs^+ cation interacts with every individual carbon atoms of C_n^{2-}. The geometries of the large Cs^+ being lightly embraced by a C_n^{2-}dianion have the maximum yield of electrostatic energy, and the negative charge of the carbon chain is stabilized.

3.3. Vibrational Frequencies. According to the vibrational frequencies and intensities of ground-state CsC_n^- (n = 3−10) clusters compiled in Table 4, the highest frequencies are 1757, 2073, 1841, 2165, 1913, 2165, 2002, and 2182 (cm^{-1}) for n = 3−10, respectively. Shown in Figure 5 is a plot of the highest frequencies of ground-state CsC_n^- (n = 3−10) versus n (CsC^- and triangle CsC_2^- not considered). One can see that the highest frequencies display a pattern of odd/even alternation. The frequency of an even-n structure is larger than that of the neighboring odd-n isomers, and the value of frequency increases with a rise in n. It seems that the odd/even pattern can be qualitatively understood based on the variation in stability of the clusters. The clusters with even n are more stable than those

TABLE 3: Optimized Geometrical Parameters of Ground-State CsC_n^- ($n = 1-10$) Clusters (Bond Lengths in angstroms and Bond Angles in degrees)

	CsC_{10}^-	CsC_9^-	CsC_8^-	CsC_7^-	CsC_6^-	CsC_5^-	CsC_4^-	CsC_3^-	CsC_2^-	CsC^-
$Cs-C_1$	4.024	3.915	3.856	3.660	3.571	3.642	3.282	3.599	3.095	3.230
$Cs-C_2$	3.677	3.570	3.515	3.364	3.295	3.325	3.086	3.408		
$Cs-C_3$	3.487	3.432	3.324	3.330	3.192	3.319				
$Cs-C_4$	3.528	3.384	3.334	3.216						
$Cs-C_5$	3.486	3.507								
C_1-C_2	1.257	1.267	1.255	1.271	1.254	1.283	1.248	1.305	1.270	
C_2-C_3	1.347	1.336	1.356	1.338	1.368	1.315	1.397			
C_3-C_4	1.239	1.264	1.236	1.285	1.234					
C_4-C_5	1.348	1.307	1.356							
C_5-C_6	1.236									
$C_1-C_2-C_3$	168.096	169.482	166.840	170.221	165.877	171.949	164.620	175.301		
$C_2-C_3-C_4$	168.920	162.044	166.415	153.636	160.956	156.498				
$C_3-C_4-C_5$	155.171	165.881	157.082	167.381						
$C_4-C_5-C_6$	160.455	147.609								

with odd n, and there is bond strengthening in the case of the former. This alternating pattern of frequency is consistent with the stability of even-n clusters.

3.4. Incremental Binding Energy. Listed in Table 5 are the total energy, atomization energy (ΔE_a), incremental binding energy (ΔE^I), and electron affinity (EA)[53] of ground-state CsC_n^- ($n = 1-10$).

The incremental binding energy (ΔE^I) which is the atomization energy difference (ΔE_a) of adjacent clusters can also reflect the relative stability of anionic clusters (Table 4).[56] It is expressed as

$$\Delta E^I = \Delta E_a(CsC_n^-) - \Delta E_a(CsC_{n-I}^-)$$

where ΔE_a is defined as the energy difference between a molecule and its component atoms:

$$\Delta E_a = nE(C) + E(Cs) - E(CsC_n^-)$$

As shown in Figure 6, the ΔE^I values of CsC_n^- vary according to a pattern of odd/even alternation: big ΔE^I when n is even and small ΔE^I when n is odd. Because a larger ΔE^I value implies a more stable CsC_n^- structure, one can deduce that the even-n CsC_n^- clusters are more stable than the odd-n ones. The odd/even alternation of incremental binding energy (ΔE^I) is consistent with the experimental observation of Gupta and Krishnamurthy on CsC_n^- ($n = 1-10$) yields.[10]

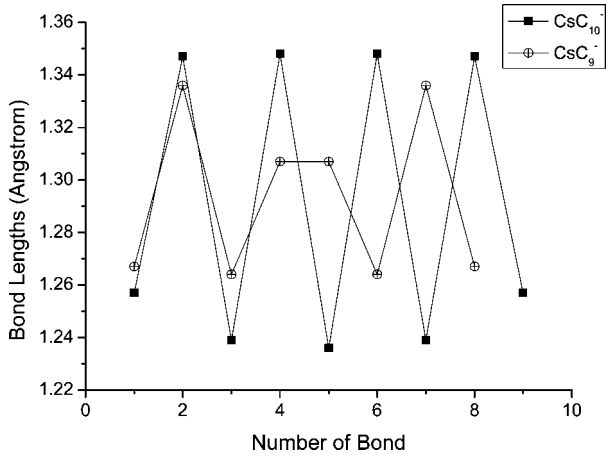

Figure 4. C−C bond lengths of ground-state CsC_9^- and CsC_{10}^- clusters vs the number of the bond (as counted from top to bottom in Figure 3).

3.5. Electron Affinity. The electron affinity of a neutral molecule is the binding energy of an electron attached to the neutral molecule[57] and can be defined as

$$EA = E(\text{optimized neutral}) - E(\text{optimized anion})$$

A higher EA means that more energy is released when an electron is added to a neutral molecule, and the generation of the corresponding anion is more readily done. Figure 7 depicts

TABLE 4: Vibrational Frequencies (cm^{-1}) and Intensities (km/mol) of Ground-State CsC_n^- ($n = 1-10$) Clusters

clusters	vibrational frequencies and intensities (in parentheses)
CsC^-	188 (48)
CsC_2^-	187 (3), 219 (28), 1756 (71)
CsC_3^-	66 (11), 116 (39), 233 (15), 416 (14), 1197 (1), 1757 (73)
CsC_4^-	136 (11), 186 (93), 242 (45), 295 (17), 404 (0), 466 (0), 876 (6), 1889 (19), 2073 (35)
CsC_5^-	74 (18), 96 (15), 136 (21), 187 (20), 357 (19), 389 (9), 418 (51), 449 (105), 791 (237), 1439 (0), 1736 (118), 1841 (99)
CsC_6^-	86 (18), 118 (63), 118 (49), 179 (0), 264 (0), 296 (6), 429 (1), 455 (11), 501 (0), 525 (80), 704 (2), 1154 (52), 1924 (15), 2041 (130), 2165 (0)
CsC_7^-	75 (16), 80 (49), 97 (46), 141 (13), 164 (0), 191 (0), 363 (4), 384 (0), 386 (0), 393 (38), 447 (1), 499 (0), 673 (0), 1048 (57), 1559 (0), 1607 (280), 1874 (50), 1913 (12)
CsC_8^-	55 (22), 65 (47), 70 (34), 124 (16), 163 (0), 190 (16), 269 (9), 284 (2), 389 (0), 400 (11), 497 (1), 502 (0), 506 (12), 508 (135), 614 (0), 943 (73), 1303 (9), 1949 (66), 2018 (86), 2157 (75), 2165 (544)
CsC_9^-	49 (21), 50 (43), 53 (14), 99 (25), 127 (0), 151 (7), 204 (15), 207 (4), 345 (0), 349 (2), 378 (0), 391 (5), 425 (18), 440 (0), 463 (0), 490 (2), 601 (0), 875 (77), 1221 (11), 1522 (401), 1691 (275), 1896 (62), 1960 (291), 2002 (41)
CsC_{10}^-	41 (26), 42 (7), 45 (42), 84 (22), 100 (0), 118 (11), 197 (14), 203 (0), 272 (0), 277 (4), 370 (3), 371 (1), 441 (143), 455 (0), 511 (34), 511 (77), 511 (0), 514 (5), 569 (2), 815 (63), 1116 (19), 1392 (0), 1952 (68), 2001 (163), 2121 (393), 2159 (55), 2182 (962)

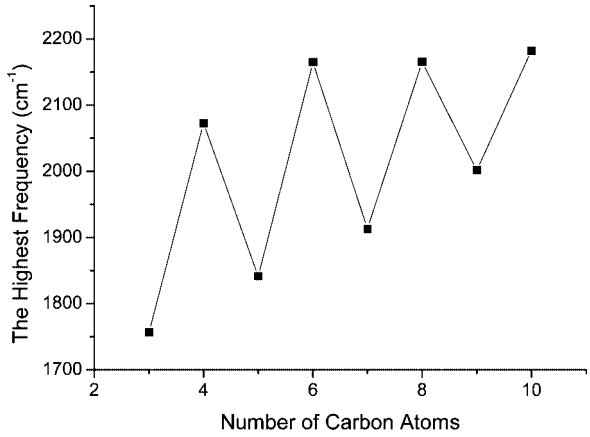

Figure 5. Highest frequencies of ground-state CsC_n^- ($n = 3-10$) clusters vs the number of carbon atoms (n).

TABLE 5: Electronic State, Total Energy (au), Atomization Energy ΔE_a (au), Incremental Binding Energy ΔE^I (au), and Electron Affinity EA (eV) of Ground-State CsC_n^- ($n = 1-10$)

cluster	state	total energy	ΔE_a	ΔE^I	EA
CsC^-	$^3\Sigma^-$	−57.821181	0.086851		1.308092
CsC_2^-	$^1A_1$	−95.973539	0.381972	0.295121	1.277156
CsC_3^-	$^3B_2$	−134.053667	0.604863	0.222891	0.974615
CsC_4^-	$^1A_1$	−172.186036	0.879994	0.275131	1.834166
CsC_5^-	$^3B_1$	−210.250475	1.087196	0.207202	1.224230
CsC_6^-	$^1A_1$	−248.387090	1.366575	0.279379	2.641420
CsC_7^-	$^3B_1$	−286.447246	1.569493	0.202918	2.025066
CsC_8^-	$^1A_1$	−324.571375	1.836385	0.266892	3.124887
CsC_9^-	$^3B_1$	−362.633893	2.041666	0.205281	2.597394
CsC_{10}^-	$^1A_1$	−400.748515	2.299051	0.257385	3.362936

the variation of EA versus the number of carbon atoms in ground-state CsC_n ($n = 2-10$) clusters. There is a parity effect on the EA curve: EA values of even-n clusters are higher than those of adjacent odd-n cluster(s); an electron attached to an even-n CsC_n is therefore more strongly bound (higher in EA) than that attached to an odd-n CsC_n. In other words, odd-n CsC_n^- can lose an electron more easily than even-n CsC_n^-. This feature is consistent with the experimental observation of Gupta and Krishnamurthy that even-n CsC_n^- are more abundant than odd-n CsC_n^-.[10] The odd/even alternation can be reasoned based on the relative stability of CsC_n and CsC_n^- clusters: even-n CsC_n^- are more stable than odd-n CsC_n^-, and for neutral CsC_n most of the odd-n and even-n members display similar stability (Figure 6).[22]

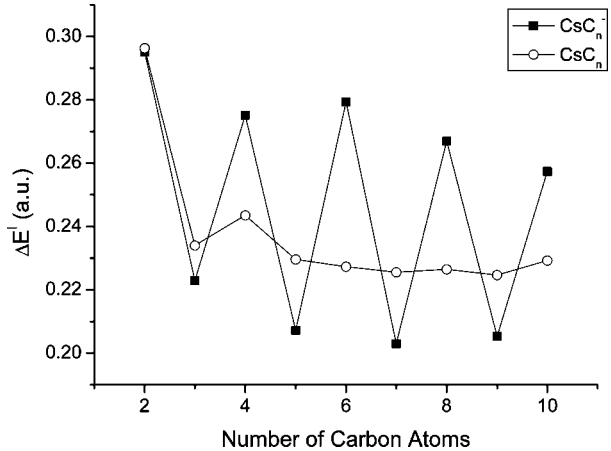

Figure 6. Incremental binding energies (ΔE^I) of ground-state CsC_n^- ($n = 1-10$) and CsC_n ($n = 1-10$) clusters vs the number of carbon atoms (n).

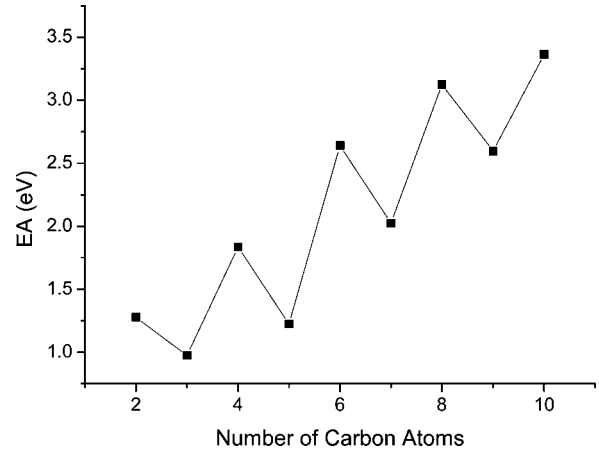

Figure 7. Electron affinity of ground-state CsC_n ($n = 2-10$) clusters vs the number of carbon atoms (n).

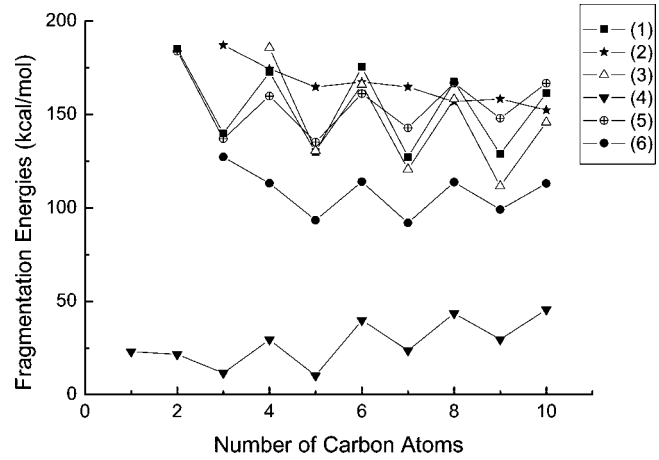

Figure 8. Fragmentation energies vs the number of carbon atoms (n).

3.6. Dissociation Channels. Due to location variation of the Cs atom and C_n, the possible dissociation channels of CsC_n^- ($n = 1-10$) could be complex. It is not our intention to characterize in this work the reaction pathways and transition states for fragmentation. What we want to do is to evaluate the relative stability of clusters in terms of fragmentation energy based on hypothetical reactions (Figure 8). The six dissociation channels can be divided into two categories. They are reactions 1−3 with C, C_2, and C_3 generation, and reactions 4−6 with Cs, CsC, and CsC_2 generation.

$$CsC_n^- \rightarrow CsC_{n-1}^- + C \quad (1)$$

$$CsC_n^- \rightarrow CsC_{n-2}^- + C_2 \quad (2)$$

$$CsC_n^- \rightarrow CsC_{n-3}^- + C_3 \quad (3)$$

$$CsC_n^- \rightarrow C_n^- + Cs \quad (4)$$

$$CsC_n^- \rightarrow C_{n-1}^- + CsC \quad (5)$$

$$CsC_n^- \rightarrow C_{n-2}^- + CsC_2 \quad (6)$$

Fragmentation energies of reactions 1 and 3 exhibit distinct odd/even alternation, and the dissociation energies of CsC_n^- with even n are always larger than those with odd n. The results

are in accord with the observation that CsC_n^- anions with even n are relatively more stable. In reaction 2, the loss of a C_2 fragment does not cause significant change in parity of the parent anionic clusters, and the alternation effect is less apparent. Reaction 4 with the loss of a Cs atom also shows a tendency of odd/even alternation ($n = 2-10$), and the energy for dissociation is the lowest among the six reactions. In other words, it is easier to break a Cs−C ionic bond than a covalent C−C bond and the loss of a cesium atom should be the dominant pathway for CsC_n^- ($n = 1-10$) dissociation. It is worth pointing out that in collision-induced dissociation (CID) observation, C_n^- is the most abundant anion in fragmentation.[10] In photoelectron spectroscopic studies[58,59] and theoretical investigation,[60] C_n^- show odd/even alternation similar to that of CsC_n^- clusters both in intensity and electron affinity. The dissociation energy of reactions 5 and 6 that involve the loss of CsC and CsC_2, respectively, exhibits a similar pattern of odd/even alternation ($n = 4-10$ in the case of reaction 6). Overall, the energy required for CsC_n^- dissociation is bigger in the cases of even n as compared to those of odd n.

4. Conclusions

The ground-state isomers of CsC_n^- ($n = 4-10$) show structures of a cesium atom lightly embraced by a C_n chain. For even-n CsC_n^-, the bond lengths and bond orders of the carbon chain suggest a polyacetylene-like structure. It is envisaged that the CsC_n^- ($n = 4-10$) isomers are composed of a Cs^+ cation and a C_n^{2-} dianion with the latter being electronically stabilized by the former. The trends of odd/even alternation in the highest vibrational frequency, incremental binding energy, and electron affinity suggest that the even-n clusters are more stable than the odd-n ones. The variations in stability are in good agreement with the relative intensity of CsC_n^- species observed in experimental studies.

Acknowledgment. The authors thank the National Science Foundation (Grants 20873107, 20533020, and 20423002) for financial support.

References and Notes

(1) Van Orden, A.; Saykally, R. J. *Chem. Rev.* **1998**, *98*, 2313.
(2) Weltner, W., Jr.; Van Zee, R. J. *Chem. Rev.* **1989**, *89*, 1713.
(3) Moazzen-Ahmadi, N.; Zerbetto, F. *J. Chem. Phys.* **1995**, *103*, 6343.
(4) Khanna, S. N.; Jena, P. *Chem. Phys. Lett.* **2001**, *336*, 467.
(5) Becker, S.; Dietze, H. J. *Int. J. Mass Spectrom. Ion Processes* **1988**, *82*, 287.
(6) Consalvo, D.; Mele, A.; Stranges, D.; Giardini-Guidoni, A.; Teghil, R. *Int. J. Mass Spectrom. Ion Processes* **1989**, *91*, 319.
(7) Huang, R. B.; Wang, C. R.; Liu, Z. Y.; Zheng, L. S.; Qi, F.; Sheng, L. S.; Yu, S. Q.; Zhang, Y. W. *Z. Phys. D: At., Mol. Clusters* **1995**, *33*, 49.
(8) Leleyter, M.; Joyes, P. *Surf. Sci.* **1985**, *156*, 800.
(9) Orth, R. G.; Jonkman, H. T.; Michl, J. *Int. J. Mass Spectrom. Ion Phys.* **1982**, *43*, 41.
(10) Gupta, A. K.; Krishnamurthy, M. *Phys. Rev. A* **2003**, *67*, 023201.
(11) Wang, C. R.; Huang, R. B.; Liu, Z. Y.; Zheng, L. S. *Chem. Phys. Lett.* **1995**, *237*, 463.
(12) Wang, C.-R.; Huang, R.-B.; Liu, Z.-Y.; Zheng, L.-S. *Chem. Phys. Lett.* **1995**, *242*, 355.
(13) Liu, Z. Y.; Huang, R. B.; Zheng, L. S. *Chem. J. Chin. Univ.* **1997**, *18*, 2019.
(14) Liu, Z.-y.; Huang, R.-b.; Tang, Z.-c.; Zheng, L.-s. *Chem. Phys.* **1998**, *229*, 335.
(15) Wang, H. Y.; Huang, R. B.; Chen, H.; Lin, M. H.; Zheng, L. S. *J. Phys. Chem. A* **2001**, *105*, 4653.
(16) Zhan, C. G.; Iwata, S. *J. Chem. Phys.* **1996**, *104*, 9058.
(17) Zhan, C. G.; Iwata, S. *J. Phys. Chem. A* **1997**, *101*, 591.
(18) Zhan, C. G.; Iwata, S. *J. Chem. Phys.* **1997**, *107*, 7323.
(19) Pascoli, G.; Lavendy, H. *Chem. Phys. Lett.* **1999**, *312*, 333.
(20) Pascoli, G.; Lavendy, H. *J. Phys. Chem. A* **1999**, *103*, 3518.
(21) Fisher, K.; Dance, I.; Willet, G. *Eur. Mass Spectrom.* **1997**, *3*, 331.
(22) Li, G.; Tang, Z. *J. Phys. Chem. A* **2003**, *107*, 5317.
(23) Li, G.; Xing, X.; Tang, Z. *J. Chem. Phys.* **2003**, *118*, 6884.
(24) Cao, Y.; Li, G.; Tang, Z. *Chin. Sci. Bull.* **2005**, *50*, 845.
(25) Vandenbosch, R.; Will, D. I. *J. Chem. Phys.* **1996**, *104*, 5600.
(26) Hunsicker, S.; Jones, R. O. *J. Chem. Phys.* **1996**, *105*, 5048.
(27) Gomei, M.; Kishi, R.; Nakajima, A.; Iwata, S.; Kaya, K. *J. Chem. Phys.* **1997**, *107*, 10051.
(28) Pan, L.; Rao, B. K.; Gupta, A. K.; Das, G. P.; Ayyub, P. *J. Chem. Phys.* **2003**, *119*, 7705.
(29) Largo, A.; Redondo, P.; Barrientos, C. *J. Phys. Chem. A* **2002**, *106*, 4217.
(30) Redondo, P.; Barrientos, C.; Largo, A. *Int. J. Quantum Chem.* **2004**, *96*, 615.
(31) Redondo, P.; Barrientos, C.; Cimas, A.; Largo, A. *J. Phys. Chem. A* **2004**, *108*, 212.
(32) Redondo, P.; Barrientos, C.; Cimas, A.; Largo, A. *J. Phys. Chem. A* **2003**, *107*, 6317.
(33) Redondo, P.; Barrientos, C.; Cimas, A.; Largo, A. *J. Phys. Chem. A* **2003**, *107*, 4676.
(34) Redondo, P.; Barrientos, C.; Largo, A. *J. Phys. Chem. A* **2004**, *108*, 11132.
(35) Largo, A.; Cimas, A.; Redondo, P.; Barrientos, C. *Int. J. Quantum Chem.* **2001**, *84*, 127.
(36) Largo, L.; Cimas, A.; Redondo, P.; Rayon, V. M.; Barrientos, C. *Int. J. Mass Spectrom.* **2007**, *266*, 50.
(37) Redondo, P.; Barrientos, C.; Largo, A. *J. Phys. Chem. A* **2005**, *109*, 8594.
(38) Redondo, P.; Barrientos, C.; Largo, A. *Int. J. Mass Spectrom.* **2007**, *263*, 101.
(39) Zhai, H. J.; Wang, L. S.; Jena, P.; Gutsev, G. L.; Bauschlicher, C. W., Jr. *J. Chem. Phys.* **2004**, *120*, 8996.
(40) Liu, J. W.; Chen, M. D.; Zheng, L. S.; Zhang, Q. E.; Au, C. T. *J. Phys. Chem. A* **2004**, *108*, 5704.
(41) Chen, M. D.; Li, X. B.; Yang, J.; Zhang, Q. E.; Au, C. T *Int. J. Mass Spectrom.* **2006**, *253*, 30.
(42) Dreuw, A.; Cederbaum, L. S. *J. Chem. Phys.* **1999**, *111*, 1467.
(43) *HyperChem Reference Manual*; Hypercube Inc.: Waterloo ON, Canada, 1996.
(44) Frisch, M. J.; Trucks, G. W.; Schlegel, H. B.; Scuseria, G. E.; Robb, M. A.; Cheeseman, J. R.; Montgomery, J. A., Jr.; Vreven, T.; Kudin, K. N.; Burant, J. C.; Millam, J. M.; Iyengar, S. S.; Tomasi, J. J.; Barone, V.; Mennucci, B.; Cossi, M.; Scalmani, G.; Rega, N.; Petersson, G. A.; Nakatsuji, H.; Hada, M.; Ehara, M.; Toyota, K.; Fukuda, R.; Hasegawa, J.; Ishida, M.; Nakajima, T.; Honda, Y.; Kitao, O.; Nakai, H.; Klene, M.; Li, X.; Knox, J. E.; Hratchian, H. P.; Cross, J. B.; Adamo, C.; Jaramillo, J.; Gomperts, R.; Stratmann, R. E.; Yazyev, O.; Austin, A. J.; Cammi, R.; Pomelli, C.; Ochterski, J. W.; Ayala, P. Y.; Morokuma, K.; Voth, A.; Salvador, P.; Dannenberg, J. J.; Zakrzewski, V. G.; Dapprich, S.; Daniels, A. D.; Strain, M. C.; Farkas, O.; Malick, D. K.; Rabuck, A. D.; Raghavachari, K.; Foresman, J. B.; Ortiz, J. V.; Cui, Q.; Baboul, A. G.; Clifford, S.; Cioslowski, J.; Stefanov, B. B.; Liu, G.; Liashenko, A.; Piskorz, P.; Komaromi, I.; Martin, R. L.; Fox, D. J.; Keith, T.; Al-Laham, M. A.; Peng, C. Y.; Nanayakkara, A.; Challacombe, M.; Gill, P. M. W.; Johnson, B.; Chen, W.; Wong, M. W.; Gonzalez, C.; Pople, J. A. Gaussian 03, revision D.01; Gaussian, Inc.: Wallingford, CT, 2004.
(45) Becke, A. D. *J. Chem. Phys.* **1993**, *98*, 5648.
(46) Lee, C.; Yang, W.; Parr, R. G. *Phys. Rev. B: Condens. Matter* **1988**, *37*, 785.
(47) Hay, P. J.; Wadt, W. R. *J. Chem. Phys.* **1985**, *82*, 270.
(48) Hay, P. J.; Wadt, W. R. *J. Chem. Phys.* **1985**, *82*, 299.
(49) Wadt, W. R.; Hay, P. J. *J. Chem. Phys.* **1985**, *82*, 284.
(50) Foresman, J. B.; Frisch, A. *Exploring Chemistry with Electronic Structure Methods*, 2nd ed.; Gaussian, Inc.: Pittsburgh, PA, 1996.
(51) Chuchev, K.; BelBruno, J. J. *J. Phys. Chem. A* **2004**, *108*, 5226.
(52) Chen, M. D.; Li, X. B.; Yang, J.; Zhang, Q. E.; Au, C. T. *J. Phys. Chem. A* **2006**, *110*, 4502.
(53) Dreuw, A.; Cederbaum, L. S. *Chem. Rev.* **2002**, *102*, 181.
(54) Chen, M. D.; Liu, J.; Chen, Q. B.; Zhang, Q. E.; Au, C. T *Int. J. Mass Spectrom.* **2007**, *262*, 136.
(55) Kolaski, M.; Lee, H. M.; Choi, Y. C.; Kim, K. S.; Tarakeshwar, P.; Miller, D. J.; Lisy, J. M. *J. Chem. Phys.* **2007**, *126*, 074302–1.
(56) Pascoli, G.; Lavendy, H *Int. J. Mass Spectrom. Ion Processes* **1998**, *173*, 41.
(57) Rienstra-Kiracofe, J. C.; Tschumper, G. S.; Schaefer, H. F., III; Nandi, S.; Ellison, G. B. *Chem. Rev.* **2002**, *102*, 231.
(58) Arnold, D. W.; Bradforth, S. E.; Kitsopoulos, T. N.; Neumark, D. M. *J. Chem. Phys.* **1991**, *95*, 8753.
(59) Yang, S.; Taylor, K. J.; Craycraft, M. J.; Conceicao, J.; Pettiette, C. L.; Cheshnovsky, O.; Smalley, R. E. *Chem. Phys. Lett.* **1988**, *144*, 431.
(60) Watts, J. D.; Barlett, R. J. *J. Chem. Phys.* **1992**, *97*, 3445.

JP807039J